

AIP Conference Proceedings
No. 57

**Nonlinear Dynamics
and the
Beam-Beam Interaction**
(Brookhaven National Laboratory, 1979)

Edited by
M. Month and J.C. Herrera



American Institute of Physics

SOME NUMERICAL STUDIES OF ARNOLD DIFFUSION IN

A SIMPLE MODEL

Boris V. Chirikov

Institute of Nuclear Physics, Novosibirsk 630090, USSR

and

Joseph Ford and Franco Vivaldi

School of Physics, Georgia Institute of Technology,

Atlanta, Georgia, 30332, U.S.A.

INTRODUCTION

One of the most powerful experimental techniques for studies of the deepest laws of nature related to the world of elementary particles is the so-called colliding beam devices, or storage rings, which provide the highest center-of-mass energy for a pair of accelerated particles. An important characteristic of such devices is the so-called luminosity, i.e. the rate of collisions between particles of the two beams which determines the efficiency (the rate) as well as the range of experiments available. The luminosity depends, in turn, on the intensity (the current) of the colliding beams. Besides some technical difficulties in the storage of a large number of particles, especially heavy ones, e.g. anti-protons, the principal limitations of beam intensity is due to the beam-beam interaction via their collective electromagnetic fields. This interaction is known to disrupt the beam completely above a certain critical beam current (see, e.g. Ref. 1 and papers in these Proceedings). Even much below this critical intensity the transverse dimensions of the beams are generally enlarged appreciably which results in a troublesome drop of luminosity. For the new generation of heavy particle colliding beam machines, now under design or even construction, the beam-beam interaction is expected to be an even more crucial phenomenon since there is no radiation damping in this case to stop the beam blow-up, and also in view of the enormously long life time of heavy particles in a storage ring which is required (of the order of a few days, or $\sim 10^{11}$ interactions, a truly cosmic time scale!) Thus extensive studies of the beam-beam phenomena seem to be highly in order, and even somewhat urgent we would say.

Generally, the collision of two intense bunches of particles is a very complicated dynamical process with an infinite number of degrees of freedom. There seems to be not much hope in any near future to study it either analytically or numerically. Thus, the importance of experimental work on existing, smaller storage rings must be emphasized, including model experiments with electrons to simulate the heavy particle behavior in future storage rings as, for example, recent experiments with low-energy electrons on SPEAR.²

A common analytical, as well as numerical, approach to the problem under consideration is the so-called weak-strong approximation of the beam-beam interaction. What is actually hidden behind this terminology is a dramatic simplification of the original problem by a cut in the number of degrees of freedom from infinity down to at most three. Namely, the influence of the weaker beam on the stronger one is completely ignored, and the motion of a single particle in a given field of the strong

beam is studied. Within the framework of such a weak-strong approximation a number of studies has been done (with some further simplifications) attempting to understand this simplified beam-beam interaction and to obtain some estimates for the critical intensity of the beam (the strong one in this approximation) (see these Proceedings and also Ref. 3 for example). The importance of those studies is related to the fact that the weak-strong stability of particle motion is certainly a necessary, even though obviously not sufficient, condition for the performance of colliding beam machines.

To the best of our knowledge all earlier studies were concerned with a strong instability of motion related to the so-called overlap of nonlinear resonances (see, e.g. review papers^{4,5}). Meanwhile, a much weaker instability - the so-called Arnold diffusion - is known to occur in such dynamical systems (see, e.g. the review paper 5 and references therein). This latter instability turns out to be a universal one in the sense that there is no critical perturbation strength for this instability. The perturbation influences the rate of instability only. This particular feature of the Arnold diffusion makes it especially dangerous for colliding beams of heavy particles where a very long particle life time is required. The phenomenon of Arnold diffusion has already been studied on simple models both numerically and analytically.⁶⁻⁷ The theories developed in these works seem to agree with numerical results within a factor of two, provided the perturbation is not too weak. The latter condition is essential because for a relatively strong perturbation, but of course still below the resonance overlap, only a few (minimum 3) resonances (perturbation terms) determine the diffusion rate, and those can be explicitly taken into account when evaluating the diffusion rate analytically (see Ref. 5 for details). For a weaker perturbation many resonances are involved, and analytical evaluation becomes much more complicated. We call this latter region of parameters the Nekhoroshev region (after the name of a Soviet mathematician who first has given rigorous upper estimates for the diffusion rate in this region⁸). Unfortunately due to obvious technical difficulties, his estimates seem to be much above the actual values of the diffusion rate (see Section 6).

The present paper is a brief report on our mainly numerical studies of the Arnold diffusion on a simple model developed in Ref. 6 (see Section 2). This model has no immediate relation to the beam-beam interaction because of the different types of nonlinearity and perturbation chosen, yet the phenomenon of the Arnold diffusion remains the same in both cases due to essentially the same phase space structure of both dynamical systems. Our main objective in these studies is an attempt to find a simple, semi-empirical relation for the diffusion rate in the Nekhoroshev regions. We seem to have found one (Section 5 Eq. 20) and we hope that these results will help other physicists in this interesting and important field of research.

2. DESCRIPTION OF MODEL

The model we have studied in this work had been developed and applied in Refs. 6,5. We have made only minor improvements to facilitate computation. The model is described by four dynamical variables: two coordinates (x_1, x_2) and two canonically conjugated momenta (p_1, p_2).

We specify the equations of motion in the form of a mapping:
 $(x_i, p_i) \rightarrow (\bar{x}_i, \bar{p}_i)$, $i = 1, 2$ where,

$$\begin{aligned}\bar{p}_1 &= p_1 - x_1^3 + \mu x_2 + \epsilon f(t) \\ \bar{p}_2 &= p_2 - x_2^3 + \mu x_1 \\ \bar{x}_1 &= x_1 + \bar{p}_1 \\ \bar{x}_2 &= x_2 + \bar{p}_2\end{aligned}\quad (1)$$

Here μ and ϵ are small perturbation parameters, and $f(t)$ is some driving force, typically periodic in integer time t which is actually the serial number of interactions for the Mapping (1).

To simplify understanding the model, we observe that for a sufficiently small difference $|\bar{p}_i - p_i| \ll 1$; $|\bar{x}_i - x_i| \ll 1$, which was actually the case in our studies, the Difference Equations (1) can be changed into the differential equations related to the Hamiltonian:

$$H(x_i, p_i) = \frac{p_1^2 + p_2^2}{2} + \frac{x_1^4 + x_2^4}{4} - \mu x_1 x_2 - \epsilon x_1 f(t) \quad (2)$$

Alternatively, one may consider the Mapping (1) as a particular numerical procedure to solve the equations of motion for the System (2). The important feature of this procedure is that Mapping (1) conserves phase space volume and, moreover, is a cononical mapping. This prevents a fast accumulation of computational errors. The latter result only in some bounded oscillations, or background, as we call it, which proves to be fairly low (Section 4).

The Hamiltonian (2) describes two nonlinear oscillators with a weak linear coupling (small parameter μ) and a driving force acting upon one of them (small parameter ϵ). It is interesting to mention that, in spite of a strong (quartic) nonlinearity, the anharmonicity, i.e. the amplitude of higher harmonics in the free uncoupled oscillations ($\mu = \epsilon = 0$) is less than 4%. The frequency of free oscillations, however, grows in proportion to the oscillation amplitude a_i . In particular,

$$\omega_i \approx \beta a_i; \quad i = 1, 2,$$

where

$$\beta = 0.8472. \quad (3)$$

Two types of the driving force were used:

$$f_1(t) = \cos(\Omega_1 t) + \cos(\Omega_2 t) \quad (4)$$

and

$$f_2(t) = \frac{\cos(\Omega t)}{1 - \text{Ac} \cos(\Omega t)} \quad (5)$$

For $(1 - A) \ll 1$, the latter force possesses a rich spectrum:

$$f_2(t) \approx \sum_m \frac{2e^{-\sigma m}}{\sigma} \cos(m\Omega t), \quad (6)$$

where

$$\sigma \approx \sqrt{1 - A^2}.$$

The main coupling resonance $\omega_1 = \omega_2$ ($a_1 = a_2$) has been chosen as the guiding resonance for Arnold diffusion. The term guiding resonance⁵ refers to the fact that the diffusion is going on just along this resonance, or to be more precise, along a stochastic layer around the separatrix of this resonance (see Ref. 5). The stochastic layer is formed due to driving resonances, or driving perturbation terms in Hamiltonian (2). The disposition of basic (first order) resonances is outlined in Fig. 1 for the driving force (5). In case of Force (4) only two nearest driving resonances remain.

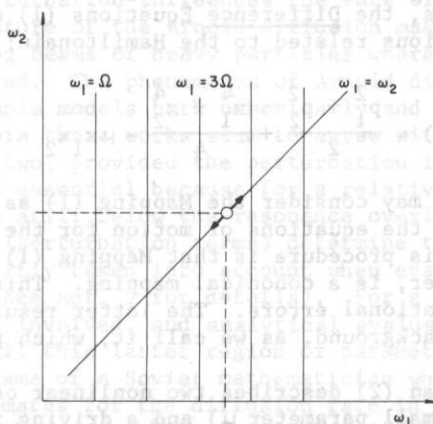


Fig. 1. A set of the first order resonances for the System (2) with driving Force (5): circle indicates location of the initial conditions; arrows show direction of the Arnold diffusion.

The initial conditions were chosen about the midpoint between two driving resonances. Typically the diffusion rate was so slow that the diffusion range, or an average shift of a trajectory was much smaller than the spacing between driving resonances, so the initial disposition of trajectories persisted during a computational run. To provide the initial location of a trajectory within the stochastic layer it was sufficient to set $x_1(0) = -x_2(0)$ ($p_1(0) = p_2(0) = 0$). Under opposite conditions: $x_1(0) = x_2(0)$ the trajectory started near the center of the coupling resonance (see Ref. 5). Both conditions are independent of the perturbation strength which greatly simplified the computation.

The diffusion rate in energy (2) was computed. Since typically the perturbation was very small, it sufficed to take account of the unperturbed energy ($\mu = \epsilon = 0$) only.

3. COMPUTATIONAL TECHNIQUES

The iteration of Mapping (1) for various values of parameters μ , ϵ , and Ω (or Ω_1 , Ω_2) and various initial conditions was performed on the CRAY-1 computer. The code has been written in FORTRAN language in such a way as to have the innermost loop vectorized which provides a much higher computation speed. To achieve this, we ran 64 trajectories simultaneously. The computation speed was around 85 MFLOPS (millions of floating point operations per second) that is about half the maximal speed (160 MFLOPS). The computation time for one iteration and one trajectory was about $0.34 \mu\text{s}$, or 27 clock periods which corresponded to approximately 3.7 minutes of CPU time for a typical run of 10^7 iterations or to 18.5 minutes for a few of the longest runs of $5 \cdot 10^7$ iterations.

The sixty-four trajectories were distributed in eight groups related to eight different values of the perturbation parameter μ . Typical values of this parameter corresponded to:

$$\mu^{-1/2} = 50, 100, 150, 200, 250, 300, 350, 400;$$

and have covered a fairly wide range of the perturbation strength:

$$\mu = 4 \times 10^{-4} \text{ to } 6.3 \times 10^{-6}.$$

For a stronger perturbation the region of resonance overlap would be entered (see Section 4). The driving force small parameter ϵ was changed in proportion to μ so that the ratio ϵ/μ was constant for a particular run. Typically, $\epsilon/\mu = 0.1$ to 0.001 .

The eight trajectories of each group were chosen with slightly different initial conditions to suppress big fluctuations in Arnold diffusion by averaging the diffusion rate over all trajectories of each group. Due to the exponential local instability inside a stochastic layer, a very small variation in initial conditions was sufficient for this purpose, typically $|\Delta x_i| \sim 10^{-5}$ to 10^{-8} .

In the computation of the diffusion rate, we followed the procedure developed in Ref. 16 and described in detail in Ref. 5, namely:

$$D_k = \frac{2}{N_k(N_k-1)} \sum_{m>n} \frac{(\bar{H}_m - \bar{H}_n)^2}{(\Delta t)_k^{(m-n)}} \quad (7)$$

To compute this quantity the total motion time t_{\max} was subdivided into N_k time intervals of length $(\Delta t)_k$ each. The current value of energy $H(t)$ was then averaged over each of these intervals to give quantities \bar{H}_m . The diffusion rate for a given pair \bar{H}_m, \bar{H}_n separated by the time interval $(\Delta t)_k^{(m-n)}$ would be $(\bar{H}_m - \bar{H}_n)^2 / (\Delta t)_k^{(m-n)}$. This rate was averaged then over all combination $m \neq n$ to give Eq. (7). Two diffusion rates were computed in each run related to two different subinterval $(\Delta t)_k$, namely:

$$(\Delta t)_1 = \frac{t_{\max}}{100}; \quad N_1 = 100,$$

$$(\Delta t)_2 = \frac{t_{\max}}{10}; \quad N_2 = 10.$$

For a true diffusion process both rates must be close (to the accuracy of statistical fluctuations). If, on the other hand, there are only bounded oscillations one would expect

$$\left(\frac{D_2}{D_1}\right)_{\text{osc.}} \approx \frac{(\Delta t)_1^3}{(\Delta t)_2^3} \rightarrow 10^{-3}, \quad (8)$$

since each of the differences $(\bar{H}_m - \bar{H}_n)$ would decrease in proportion to $(\Delta t)_1/(\Delta t)_2$. For the same reason the computational value of each D in the case of bounded oscillations rapidly decreases with the motion time:

$$D_{\text{osc}} \sim t_{\text{max}}^{-3}. \quad (9)$$

Comparing the two values of D_1 and D_2 , one can get a rough idea as to the possible portion of side (non-diffusion) processes. It is clear also that the D_2 rate is the much more reliable of the two, and so all the data below correspond just to this diffusion rate D_2 .

4. NUMERICAL RESULTS

An example of the dependence of the diffusion rate (decimal logarithm of D_2) on the perturbation ($1/\sqrt{\mu}$) is plotted in Fig. 2 for the following set of parameters: $|x(0)| = 0.225$; $\Omega = 0.03466$; $A = 0.995$ [force (5)]; $\epsilon/\mu = 0.01$ with μ in the range: $1/\sqrt{\mu} = 6$ to 400, and the motion time $t_{\text{max}} = 10^3$ to $5 \cdot 10^7$ depending on perturbation. Dependence on $1/\sqrt{\mu}$ has been taken merely in analogy with a simple theory of the Arnold dissipation^{5,6}, where the quantity $1/\sqrt{\mu}$ enters the exponent and, thus, essentially determines the dependence $D(\mu)$ (see below, Section 5).

For the chosen amplitude $a = |x(0)| = 0.225$ the oscillation frequency $\omega(0) = 0.19$, and the ratio $\omega/\Omega = 5.5$, that is, the system is located between resonances of 5th and 6th harmonics of the driving force. This frequency value is sufficiently small to provide a low background. A rough estimate of the background can be gotten from the 'diffusion rate' near the center of resonance where the motion is perfectly stable for a sufficiently weak perturbation. As is seen from Fig. (triangles), the background level $D_b \approx 10^{-25}$ for the motion time $t_{\text{max}} = 10^7$. The rate D_1 in this case is $\sim 10^{-22}$, as one would expect from Estimate (8). If $t_{\text{max}} = 10^6$ the background (D_2) grows by about 2 to 4 orders of magnitude, again in rough accordance with Estimate (9). On the contrary, for initial conditions inside the stochastic layers the diffusion rate does not depend on the motion time t_{max} within a factor of 2. This difference seems to be mainly due to still appreciable fluctuations in spite of averaging over 8 trajectories. As explained at length in Ref. 5, the fluctuations are related to the complicated structure of a stochastic layer, especially its peripheral part near the layer edge. A trajectory may 'stick' here for a relatively long period of time which results in a big deviation from the average diffusion rate. This is apparently also the main cause for an always present slight difference between the two rates D_1 and D_2 . Typically, inside the stochastic layer $D_2/D_1 \approx 0.8$.

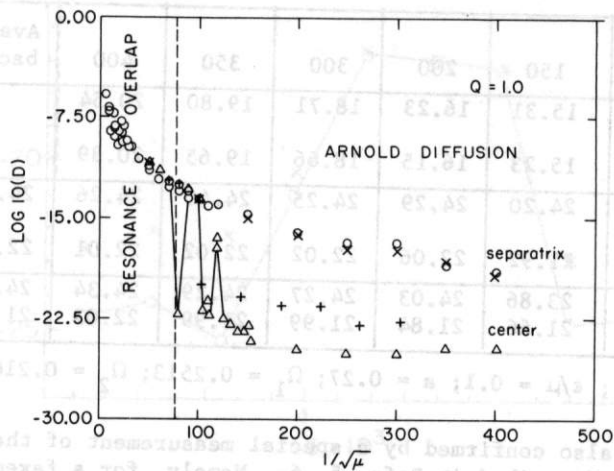


Fig. 2. Diffusion rate D vs. perturbation $1/\sqrt{\mu}$: O-inside the stochastic layer; x-same with a lower accurately reduced by a factor of 500; Δ -at the center of resonance, $t_{\text{max}} = 10^7$; + -same for $t_{\text{max}} = 10^6$.

Another estimate for the background can be obtained from runs with a single driving resonance [for the force (4)]. As is explained in detail in Ref. 5, no long-range diffusion is possible in this case. The point is that a single driving resonance would provide the diffusion only in a certain particular direction in the action or frequency plane of the system (Fig. 1). This direction does not generally, and particularly for the model under consideration, coincide with the direction of guiding resonance (and its stochastic layer). Since the width of stochastic layer is typically very small for weak perturbation the resulting motion would be of the type of bounded oscillations. In Table 1 we compare the diffusion rates for a single and two driving resonances as well as for trajectories near the resonance center with parameters given below the Table. We see that the background as determined near the resonance center and inside the stochastic layer with a single driving resonance is practically the same and much lower than the rate of Arnold diffusion. The ratio $D_2/D_1 \approx 5 \cdot 10^{-3}$ for two background runs is somewhat larger than expected from Eq. (8) but much lower than for the Arnold diffusion (first run, $D_2/D_1 \approx 0.8$). A low background value for a single driving resonance shows that the Arnold diffusion in the first run is really a long-term one, that is, its range during the motion time $t_{\text{max}} = 10^7$ is much larger than the width of stochastic layer.

Table 1. Background.

$1/\sqrt{\mu}$						Average background	
	150	200	300	350	400		
2 driving resonances	15.31	16.23	18.71	19.80	20.54	-	$-\log D_2$
	15.23	16.15	18.66	19.65	20.39	-	$-\log D_1$
1 driving resonance	24.20	24.29	24.25	24.40	24.26	24.28	$-\log D_2$
	21.92	22.06	22.02	22.02	22.01	22.01	$-\log D_1$
resonance center	23.86	24.03	24.27	24.29	24.34	24.16	$-\log D_2$
	21.66	21.84	21.99	21.99	22.03	21.90	$-\log D_1$

$$t_{\max} = 10^7; \quad \epsilon/\mu = 0.1; \quad a = 0.27; \quad \Omega_1 = 0.2513; \quad \Omega_2 = 0.2167$$

It is also confirmed by a special measurement of that width using a procedure described in Refs. 5, 6. Namely, for a fixed perturbation the initial conditions were chosen according to the expression $(p_1(0) = p_2(0) = 0)$:

$$x_1(0) = a + d_i; \quad x_2(0) = a - d_i, \quad (10)$$

where i stands for the serial number of a trajectory group. If $d = 0$ the trajectory starts at the resonance center and reveals only a background 'diffusion' as we have seen above. Yet as d increases, a trajectory eventually crosses the stochastic layer that is immediately obvious from numerical data by a 'jump-up' of the diffusion rate. An example of the dependence of diffusion rate on the shift d is plotted in Fig. 3. The stochastic layer is clearly seen at $d \approx 4.5 \times 10^{-3}$, in reasonable agreement with the theoretical prediction $d_1 = \sqrt{\mu} = 5 \cdot 10^{-3}$. The layer width $\Delta d \approx 4 \cdot 10^{-4}$ is also close to the expected value $\Delta d \approx 4.3 \times 10^{-4}$ according to the expression derived in Ref. 5. Note that the diffusion rate drops by about 8 orders of magnitude (!) at both edges of the layer. According to Ref. 5, the layer width in energy is related to (Δd) by a simple expression:

$$\Delta H = a^2 \cdot d \cdot \Delta d. \quad (11)$$

Whence the time interval required for the diffusion to reach across the layer is

$$T_\ell \sim \frac{(\Delta H)^2}{D} \sim 10^3. \quad (12)$$

Numerical estimate is given for the parameters used in Fig. 3. Time interval T_ℓ is much less than the motion time $t_{\max} = 10^7$, so that the diffusion is spreading along the stochastic layer at a distance 100 times as much as the layer width. However for this run the relative change in energy is only $\sim 1\%$, and even 4 times less in amplitude and in frequency $\omega(a)$. This results in only $\sim 1\%$ relative change in detuning $\delta\omega = \Omega_1 - \omega \approx \omega - \Omega_2$.

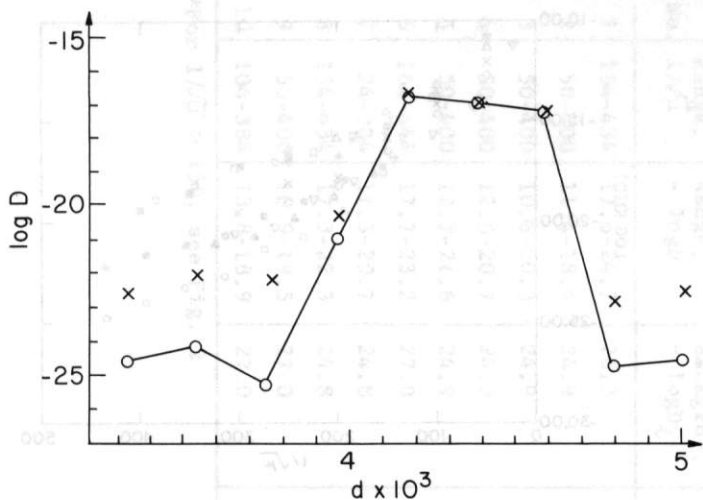


Fig. 3. Diffusion rate vs. initial conditions: $d = [x_1(0) - x_2(0)]/2$; $p_1(0) = p_2(0) = 0$; $1/\sqrt{\mu} = 200$; $\epsilon/\mu = 0.1$; $a = 0.2$; $t_{\max} = 10^7$; $\log D_1 - X$; $\log D_2 - o$.

Coming back to Fig. 2 we see that even for the weakest perturbation with $1/\sqrt{\mu} = 400$, the background is more than 5 orders of magnitude lower as compared to the rate of Arnold diffusion inside stochastic layer (Fig. 2). However, for a sufficiently strong perturbation ($1/\sqrt{\mu} \leq 80$) the diffusion rate near the resonance center 'jump up' by almost 10 orders of magnitude (!) and attains that level inside the stochastic layer. This simply means that the resonance center has become completely destroyed by a strong resonance overlap whose border is marked in Fig. 2 by the dashed vertical line as evaluated according to Ref. 5 (there, see Section 4.1). This line, thus, divides the whole perturbation range into two regions—the resonance overlap, or a strong stochasticity, and the Arnold diffusion, or a weak but universal instability. Note, that there is no obvious change in the dependence $D(\mu)$ between these two regions in spite of a quite different mechanism of the diffusion. This allows us to describe diffusion in both regions by a single expression except, perhaps, under the very strong perturbation at the leftmost part of the plot in Fig. 2 (see Section 5).

Another set of data is plotted in Fig. 4. It corresponds to 10 runs with parameters given in Table 2. The quantity $\delta\omega$ is the detune between the oscillation frequency $\omega(0)$ and that of the nearest driving resonance. In all runs of Table 2 but the first the two detunes, which are related to the two nearest driving resonances, are equal. If they are not equal, the bigger of the two values should be taken. The point is that, as was explained above in this section (for more detail see Refs. 5, 6), a long-range diffusion can be provided only by at least two driving resonances. Hence, if the influence of two resonances is different (due to a different detune, for example), the diffusion will be determined by the weaker one (with a larger detune).

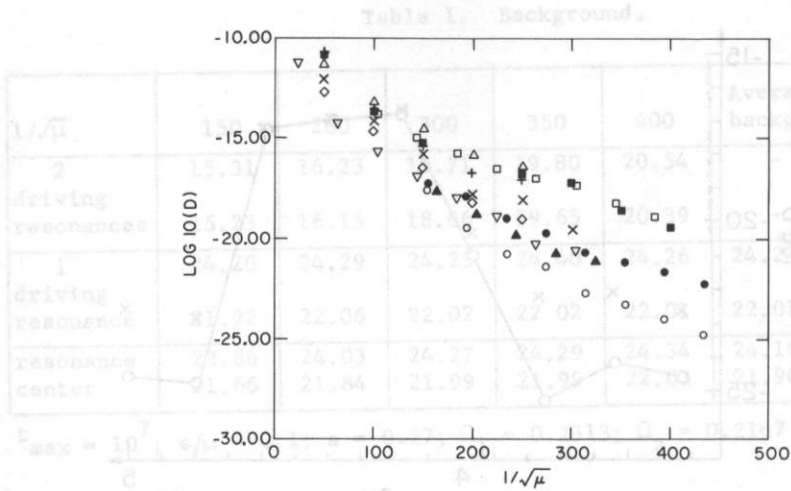


Fig. 4. Diffusion rate D vs. perturbation $1/\sqrt{\mu}$, parameters of trajectories are given in Table 2.

A large dispersion of points between runs in Fig. 4 is obviously due to the variation of the model parameters for these different runs. Since our model has no immediate relation to the problem of the beam-beam interaction in which we are interested, the 'raw' data presented in Fig. 4 are only of a minor importance. We need thus to trace some regularities in this raw material to get rid of the peculiarities of the particular model under consideration.

5. SCALING

We may start with an explicit expression for the rate of Arnold diffusion in our model as derived in Ref. 5:

$$D \approx \frac{(\pi a \omega f_m)^2}{3L\Omega_\mu} \cdot e^{-\frac{\pi|\delta\omega|}{\Omega_\mu}}, \quad (13)$$

where f_m is the Fourier amplitude for the nearest harmonic of the driving force $f(t)$, $\Omega_\mu \approx 0.85\sqrt{\mu}$ the frequency of small phase oscillations on the guiding resonance⁵, and L is some logarithmic factor which for our rough estimates may be considered as a constant. The physical meaning of the first factor is very simple and transparent. Indeed, the quantity $a\omega f_m \sim \epsilon f_m \dot{x}$ gives the order of magnitude of the driving force power responsible for the diffusion in energy. Further, since an elementary change ΔH happens each halfperiod of the phase oscillations (see Ref. 5), that is on time scale $T_\mu \sim 1/\mu$, one would expect $\Delta H \approx \epsilon f_m a \omega T_\mu$, or for the diffusion rate

$$D \sim \frac{(\Delta H)^2}{T_\mu} \approx \frac{(\epsilon f_m a \omega)^2}{\Omega_\mu}, \quad (14)$$

Table 2. Parameters of trajectories related to Fig. 4.

No.	Range, $1/\mu$	Range, $-\log D$	Backgrd*, $-\log D \zeta$	t_{\max}	$\frac{\epsilon}{\mu}$	a	A	$\frac{m}{\Omega}$	$\frac{\Omega_1}{\Omega_2}$	$ \delta\omega $	Symbol in Fig. 4	Comments
1	154-434	17.6-24.7	26.3	$5 \cdot 10^7$	0.01	0.27	-	-	29/25	0.0226	\emptyset	Force (4)
2	50-400	11.4-18.4	24.9	10^7	0.01	0.225	0.995	6.5	-	0.0147	Δ	Force (5)
3	50-400	10.8-20.3	24.9	10^7	0.01	0.225	0.995	4.5	-	0.0212	+	"
4	50-400	12.0-20.7	24.9	10^7	0.01	0.295	0.995	3.5	-	0.0272	x	"
5	50-400	12.7-21.6	24.9	10^7	0.01	0.295	0.98	5.5	-	0.0173	\diamond	"
6	164-444	17.7-23.2	27.0	$5 \cdot 10^7$	0.001	0.225	0.995	5.5	-	0.0173	∇	"
7	24-304	11.3-20.7	24.8	10^7	0.001	0.225	0.995	5.5	-	0.0173	\times	"
8	154-434	17.3-22.3	24.8	10^7	0.001	0.265	0.995	5.5	-	0.0177	\otimes	"
9	50-400	10.9-19.5	27.0	$5 \cdot 10^7$	0.01	0.225	0.995	5.5	-	0.0173	Y	"
10	104-384	13.8-18.9	27.0	$5 \cdot 10^7$	0.01	0.225	0.995	5.5	-	0.0173	\boxtimes	"

*For $1/\mu > 150$, see Fig. 2

in accordance with explicit Relation (13). Note, that the symbol \propto here means proportionality rather than order of magnitude (symbol \sim), since obviously an exponential factor is present. Nevertheless, this estimate for the factor is part of the exponential term seems to be fairly general, and we may try to rescale the numerical data making use of the dependence in Relationship (14). Namely, let us introduce the reduced diffusion rate D^* according to the relation

$$D^* = \frac{D/\bar{\mu}}{\epsilon^2 f^2 a^4} = D/\epsilon^2 f^2 a^4 \mu^{3/2} \left(\frac{\epsilon}{\mu}\right)^2. \quad (15)$$

The latter expression takes into account the fact that in a single run $\epsilon/\mu = \text{constant}$, and so besides a constant factor only dependence on μ is to be introduced in rescaling.

As was observed in Refs. 5, 6, relation (13) does not hold for a sufficiently weak perturbation (see Fig. 5 below), so the exponent in

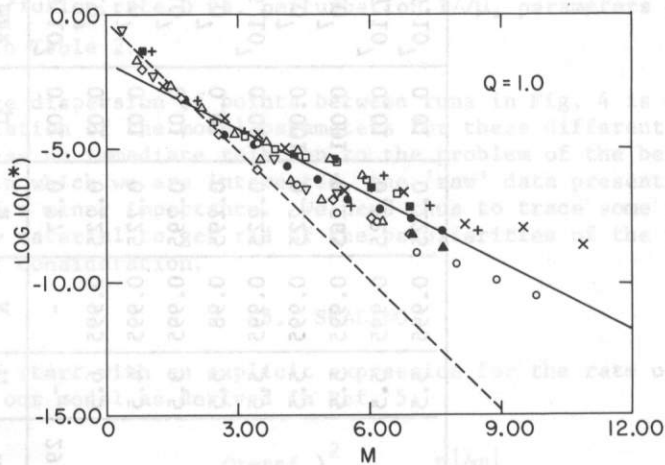


Fig. 5. Dimensionless diffusion rate D^* vs. rescaled perturbation $M = |\delta\omega|/\sqrt{\mu}$. Dashed line shows dependence given in Eq. (13), and the solid line is the least square fit of the data to the Relation (16), using $Q = 1$.

Eq. (13) has to be changed somehow. At this point we may try to make use of some rough estimates derived in Ref. 5 (see also Ref. 9 for a simplified version) which may be represented in our case as follows:

$$D^* = A \cdot \exp \left[-B \cdot \left(\frac{F}{\Omega \mu}\right)^{1/Q} \right] \quad (16)$$

where A , B , f and Q are some constants independent of the perturbation. Since D^* is a rescaled diffusion rate, the factor A is dimensionless and would be expected to be of the order unity. Parameter F may be chosen

to have the dimensions of frequency in order to make factor B dimensionless. Note that the analytical estimate (13) is also of the type of Eq. (16) with

$$A = \frac{\pi^2 B}{3L} \approx 0.56 ; B = \pi ; F = |\delta\omega| ; Q = 1 ,$$

where $L \approx 5$ is assumed for $1/\sqrt{\mu} \sim 100$, and relations $\omega = \beta a$ and $\Omega_{\mu} = \beta/\mu$ are taken into account.⁵ Relation of the type (16) follows also from Nekboroskev's estimates in Ref. 8. Since the Relation (13) describes the Arnold diffusion fairly well for a relatively large perturbations^{5,6}, it seems plausible to assume $F = |\delta\omega|$ also for a weaker perturbation. In other words, we may rescale the perturbation as well by introducing into Eq. (16) a dimensionless quantity:

$$M = \frac{|\delta\omega|}{\Omega_{\mu}} = \frac{|\delta\omega|}{\beta/\mu}$$

Now we may rescale numerical data to the variables D^* and M and try to fit them to Eq. (16). An example of rescaled data for the 10 runs listed in Table 2 is given in Fig. 5 using coordinates $\log D^*$ and M for $Q = 1$. The dashed line represents Relation (13) which is valid only for $M \leq 3$.

From comparison of Fig. 4 with Fig. 5, it is clearly seen that the dispersion of numerical points has been considerably reduced by rescaling. Thus, Eq. (16) at least represents some partial dependence of the diffusion rate on the model parameters. (Note the difference in scale of the vertical axis on the two Figs.). To find the optimal values of the parameters A, B and Q in Relation (16), a least squares fit of the numerical data was done in the following way. For a given value of Q the pairs of quantities $\log D^*$ and $M^{1/Q}$ for all the 10 runs in Table 2 have been fitted to a straight line corresponding to the Relation (16), each fit giving two parameters A and B in dependence on Q value. The quality of a fit is characterized by the root-mean-square deviation

$$S = \sqrt{\langle (\log D^* - \log D_F^*)^2 \rangle} , \quad (18)$$

where D^* are computational data and where D_F^* is related to Eq. (16). It is convenient to introduce another characteristic of dispersion

$$R = 10^S = 10 \sqrt{\langle \left(\lg \frac{D^*}{D_F^*} \right)^2 \rangle} , \quad (19)$$

which represent a certain average ratio $\langle D^*/D_F^* \rangle$ (or vice versa $\langle D_F^*/D^* \rangle$, of course). The results of the fit are summarized in Table 3.

Table 3. The least square fit of data in Table 2 to the Relation (16).

Q	1	2	3	4	5	6	7	8
A	0.0155	25.8	2.94×10^4	3.06×10^7	3.06×10^{10}	3.01×10^{13}	2.94×10^{16}	2.84×10^{19}
B	1.92	7.86	14.5	21.2	28.1	34.9	41.8	48.6
R	4.97	3.87	3.95	4.09	4.21	4.31	4.39	4.45

The ratio R characterizing the dispersion of numerical points (see Fig. 5) is not very sensitive to the value of Q , especially for a large Q , but factor changes drastically with Q . Since $A \sim 1$ is expected, as mentioned above, we have only to choose between $Q = 1$ and $Q = 2$. The value $Q = 2$ seems to be better in regard to a lower dispersion R and a reasonable value of A . Thus, we would suggest the following estimate for the rate of Arnold diffusion

$$D^* \approx 26 \cdot \exp(-7.9 \times \sqrt{M}) . \quad (20)$$

In Fig. 6 numerical data are plotted in coordinates $\log D^*$ and \sqrt{M} , the straight line representing Relation (20). Surprisingly, this relation describes satisfactorily also the region $M < 3$ where more accurate estimate (13) is applicable (comp. Fig. 5), and even the resonance overlap region. The latter would correspond roughly to $\sqrt{M} \leq 1.3$ except trajectories No. 3 and 4 (see Table 2 and Fig. 2).

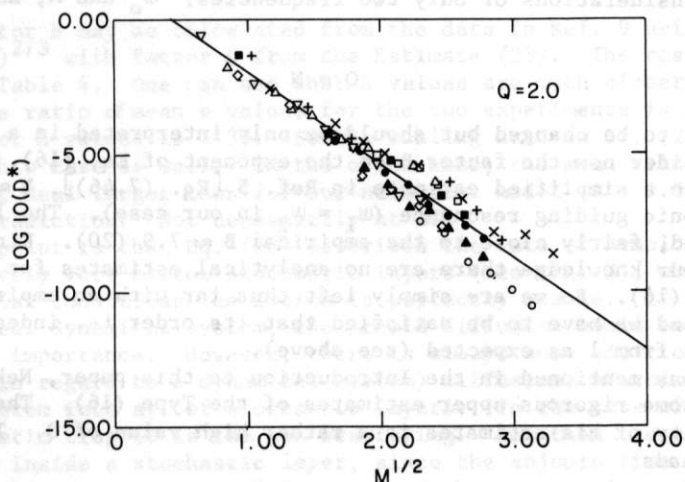


Fig. 6. Same as in Fig. 5 for $Q = 2$.

For another set of 10 runs with different values of the parameters the least dispersion was obtained also for $Q = 2$ with $A = 42.1$ and $B = 8.2$ which is rather close to the rough estimate given by Eq. (20). The minimal dispersion $R = 3.21$ was still less in the latter case (comp. Table 3). If one should try to fit original numerical data (in coordinates $\log D$ and $1/\sqrt{\mu}$) as plotted in Fig. 4, one would obtain the minimal $R \approx 30$ for both sets of runs. On the other hand, the minimal dispersion for a single run fit would be $R \approx 1.13$ only. So, the above mentioned dispersion $R \approx 3$ characterizes the accuracy of a simplified Estimate (20).

6. DISCUSSION

The main question to be discussed is whether Estimate (20) describes Arnold diffusion only for the model under consideration, and moreover, only in the restricted range of parameters actually studied numerically,

or can one hope to apply Eq. (20) in a more general situation. This question may be answered partly via a comparison of the empirical parameters in Eq. (20) with the analytical consideration of Ref. 5 (see also Ref. 9). Let us consider first the most important parameter Q . According to Ref. 5, it is equal to the number N of basic frequencies of the unperturbed system whose combinations give rise to a dense set of driving resonances. It is precisely these higher order resonances which increase the diffusion rate as compared to the simple Estimate (13) (see Fig. 5). Even though their amplitudes are much smaller than for the first order resonances (Fig. 1) on which Eq. (13) is based, they are much closer so that the corresponding detune $|\delta\omega|$ is much smaller. Eventually, as the perturbation decreases, just those high order resonances determine the diffusion rate (for more details see Refs. 5, 9). Since in the model under consideration there are 3 basic frequencies $[\omega_1, \omega_2, \Omega, \text{Force (5)}]$, Relation (20) with $Q = 2$ seems to contradict at the first glance with the conclusion in Ref. 5, 9. However, the two frequencies in our computation are very close, especially for a weak perturbation $\omega_1 \approx \omega_2 \approx \omega_0$. Hence, the high order resonances are essentially related to the considerations of only two frequencies: ω_0 and Ω , and the general relation

$$Q = N \quad (21)$$

needs not to be changed but should be only interpreted in a proper way.

Consider now the factor B on the exponent of Eq. (16). Again, according to a simplified estimate in Ref. 5 [Eq. (7.46)], $B \approx 2\pi$ for a low harmonic guiding resonance ($\omega_1 = \omega_2$ in our case). The latter value is, indeed, fairly close to the empirical $B \approx 7.9$ (20). Finally, to the best of our knowledge there are no analytical estimates for the factor A in Eq. (16). So we are simply left thus far with an empirical value $A \approx 26$, and we have to be satisfied that its order is, indeed, not much different from 1 as expected (see above).

As was mentioned in the Introduction to this paper, Nekhoroshev obtained⁸ some rigorous upper estimates of the Type (16). The main peculiarity of his estimates is a rather high value of Q . This best result reads:

$$A = \frac{3N^2 - N + 8}{4} = 4.5 \quad (22)$$

where numerical value is given for $N = 2$. This value seems to contradict with our numerical results since the corresponding factor A would be incomprehensibly big (see Table 3).

Summarizing, we have reason to believe that Estimate (20) may have a wider application than to just the simple immediate model from which it has been obtained.

Let us try to apply our estimate to a rather different system, namely a particle in a magnetic trap. The alleged Arnold diffusion of electrons in two different experiments was analysed in Ref. 9 using a rough estimate

$$\tau\nu^2 \sim \exp(b/\Omega_\phi^{1/3}), \quad (23)$$

where τ is electron lifetime; ν dimensionless strength of driving resonances due to the azimuthal variation of the magnetic field; $Q = N = 3$ since there is no special relation between the basic frequencies, Larmor frequency $\omega = 1$, and the frequency of phase oscillations on a guiding resonance

$$\Omega_{\perp} \sim \exp(1/2\epsilon), \quad (24)$$

with some small adiabaticity parameter ϵ . Now we may rescale the perturbation as was done in Section 5 for our simple model, namely:

$\Omega_{\perp} \rightarrow \Omega_{\perp}/|\delta\omega|$, where mean detune ($\delta\omega$) is determined now by the lowest drift frequency of an electron $\Omega_{\phi} \sim (\rho/\ell)^2$ with ρ equal to the electron Larmor radius, and ℓ the scale of the magnetic field, whence:

$$\tau\nu^2 \sim \exp \left[-B \frac{\rho}{\ell} \frac{2/3}{e^{2\epsilon}} \right]. \quad (25)$$

A new factor B may be calculated from the data in Ref. 9 using relation: $B = b(\ell/\rho)^{2/3}$ with factor b from the Estimate (23). The results are shown in Table 4. One can see that B values are much closer than those of b . The ratio of mean b values for the two experiments is 2.33, whereas that for B values is 1.35. So the scaling used in Eq. (20) seems to work in this case as well. On the other hand, the mean value $\langle B \rangle = 12.9$ is a great deal larger than for our numerical model ($B = 7.9$). Is it a real contradiction? Not necessarily at all!

The point is that Eq. (20) describes the rate of Arnold diffusion in relatively very narrow stochastic layers (see Fig. 3), whereas for most initial conditions the motion is perfectly stable. If it would be so in a real dynamical system, the Arnold diffusion would be of no practical importance. However, there is always some additional 'external' (in regard to a dynamical system) diffusion, or noise, which brings system into all of stochastic layers. In the case of electrons in a magnetic trap it is the gas scattering. But then the average diffusion inside a stochastic layer, since the sojourn time inside a layer amounts to only a small fraction of the motion time. The corresponding reduction of the diffusion rate may be very roughly estimated as follows. From a simple theory of the Arnold diffusion resulting in a relation like Eq. (13), it is known⁵ that the width of a stochastic layer (ω_s) is proportional to an exponential factor similar to one in the diffusion rate.

$$\omega_s \propto \exp \left(-\frac{\pi |\delta\omega|}{2\Omega_{\perp} \mu} \right).$$

The exponent in the latter expression differs from that in the diffusion rate by a factor of (1/2) only. One can draw from this comparison a very rough conclusion that the reduction of the diffusion rate due to some external noise, being proportional to the layer width, would result in an increase of the factor B in Eq. (16) by a factor 1.5. In other words the reduced diffusion rate would be roughly a product of the rate inside a layer and the layer width. The actual ratio of B

values for a electron in magnetic traps (Table 4) and for our purely dynamical model [Eq. (20)] is 1.63. Since estimate (25) is very rough and is based upon only a few experimental points (see Table 4), any recommendation of this estimate seems premature. Instead, additional studies of the Arnold diffusion in more realistic conditions are very much in order.

Table 4. Arnold diffusion in magnetic traps.

	$\frac{1}{\epsilon}$	$\frac{\ell \ell}{\rho \rho}$	b	B
1st. experiment	7.89	8.96	3.66	15.8
	6.68	6.61	4.38	15.4
	8.25	6.61	3.37	11.9
2nd. experiment	13.6	17.6	1.75	11.8
	14.5	15.5	1.51	9.4

Mean Value

12.9

ACKNOWLEDGMENT

The authors express their sincere appreciation for the assistance, stimulating conversations, and useful comments which were provided by G. Casati, G. Contopoulos, E. Courant, F. Izraelev, E. Keil, A. Lichtenberg, M. Lieberman, O. Manley, M. Month. R. Peierls, and J. Tennyson.

This work was performed under the U.S.A. - U.S.S.R. Cooperative Program on Research in the Fundamental Properties of Matter. We appreciate the assistance of the U.S. Department of Energy and the U.S.S.R. Academy of Science in making this joint research possible.

REFERENCES

1. E. Keil, "Experimental Data on the Beam-Beam Limit and Their Consequences on the Design of LEP," CERN/ISR/TH/79-32, 1979.
2. M. Wiedemann, private communication.
3. F. M. Izrailev, S. I. Mishnev, G. M. Tunaikin, "Numerical Studies of Stochasticity Limits in Colliding Beams (One-Dimensional Model)," Preprint 77-43, Institute of Nuclear Physics, Novosibirsk, 1977.
4. J. Ford, in Fundamental Problems in Statistical Mechanics, Vol. 3, Edited by E.G.D. Cohen (North-Holland, Amsterdam, 1975).
5. B. V. Chirikov, "A Universal Instability of Many-Dimensional Oscillator Systems," Physics Reports 52:5 (1979) 265.
6. G. V. Gadiyak, F. M. Izraelev, B. V. Chirikov, "Numerical Experiments on a Universal Instability in Nonlinear Oscillator Systems (The Arnold Diffusion)," Proc. 7th Int. Conf. on Nonlinear Oscillations (Berlin, 1975), Vol. II, 1, 315; "The Arnold Diffusion in a System of Three Resonances" (to be published).
7. J. L. Tennyson, M. A. Liebermann, A. J. Lichtenberg, "Diffusion in Near-Integrable Hamiltonian Systems With Three Degrees of Freedom," Memorandum No. UCB/ERL M79/1, College of Engineering, Berkeley, 1979.
8. N. N. Nekhoroshev, Usp. Mat. Nauk 32:6 (1977).
9. B. V. Chirikov, "The Problems of Motion Stability for a Charged Particle in a Magnetic Trap," Fizika Plasmy 4:3, 527 (1978).